STUDIA UNIVERSITATIS BABEŞ-BOLYAI, CHEMIA, LI, 1, 2006

ADSORPTION KINETICS OF STEARIC ACID AT THE BENZENE/WATER INTERFACE

MARIA TOMOAIA-COTISEL*

ABSTRACT. The adsorption kinetics of stearic acid from benzene solutions at the benzene/water interface was studied by using the pendant drop method. Kinetic equations for diffusion controlled adsorption and for Langmuir adsorption were tested. A theoretical approach to the dynamic interfacial pressures is developed and a new kinetic equation for the diffusion controlled kinetics is proposed, based on Ward and Tordai's diffusion equation associated with a two dimensional van der Waals state equation. It is shown that this approach describes the dynamic interfacial pressures within the limits of the experimental errors and the new equation is valid over a wide range of time and for different surfactant concentrations in oil solutions. It is also concluded that this new approach allows the calculation of diffusion coefficients, subsurface concentrations and intermolecular interaction parameters within adsorbed layers of biosurfactants at the oil/water interfaces. Obtained results are in substantial agreement with similar earlier reported data for the surfactant adsorption at liquid/liquid interfaces.

Keywords: Diffusion controlled adsorption; Langmuir adsorption kinetics; Dynamic interfacial pressures; Pendant drop method; Stearic acid; Benzene/water interface

Introduction

The adsorption of surfactant molecules at the air/water and oil/water interfaces has attracted a considerable attention in the last several decades (1-28) due to its fundamental and industrial importance (1-4, 25) as well as to its biological significance (29-32). These studies have involved various experimental techniques as well as the formulation of theoretical models for describing the adsorption kinetics of surfactants at liquid interfaces.

Generally, the adsorption of surfactant molecules from a solution to a liquid/gas (1-15) or to a liquid/liquid interface (1, 5, 16-24) occurs in two steps. Surfactant is first transported from the bulk to the subsurface by diffusion (the subsurface is a liquid layer just below the interface, belonging still to the bulk). The second step is the transfer from the subsurface to the interface, implying sometimes a transfer through a potential barrier (22, 25-28). In miscellaneous systems the controlling rate may be either the diffusion (i.e. the adsorption may be diffusion controlled), or the transfer (i.e. the adsorption is barrier-controlled). Several theoretical models have

* "Babes-Bolyai" University of Cluj-Napoca, Department of Physical Chemistry, 400028 Cluj-Napoca, Romania; mcotisel@yahoo.com

been developed for both processes, as well as for mixed adsorption mechanisms in which both steps are considered (1-6).

In the case of adsorption to a liquid/liquid interface (1, 16-24), the situation is analogous to that for the air/water interface if the solute is soluble only in one liquid phase. If the solute is soluble in water and in oil phases, then the adsorption process includes also the solute transfer across the interface into the other liquid bulk phase (16).

For example, the adsorption kinetics of some aliphatic carboxylic acids and aliphatic alcohols (6-9), like 1, 9 nonane dicarboxylic acid and 1, 9 nonane diol (6), was studied at the air/water interfaces and described by Langmuir kinetic equation, considering the adsorption and desorption rate constants. Another example is related to the adsorption of some salts of fatty acids, like sodium laurate (10-13), sodium myristate (10-12), and sodium oleate (14), from aqueous solutions to the air/water interface, which was analyzed by means of diffusion controlled kinetics. However, the very slow adsorption of fatty acids from oil phase to the oil/water interface has received only a limited attention (5).

The main goal of this work is to focus on the experimental dynamic data for the adsorption of stearic acid at the benzene/water interface and to discuss the theoretical aspects of adsorption kinetics at the oil/water interface. The experimental data are recorded in terms of the time dependent interfacial pressures, which are also known as dynamic interfacial pressures. These interfacial pressures are dependent of time and of the surfactant bulk concentration and of the surfactant interfacial adsorption. An equilibrium state is reached when the interfacial pressure is constant (18, 23, 24).

Stearic acid is a fatty acid widely used in model biomembranes (29-32) as well as in Langmuir-Blodgett films due to its increased stability in monolayers at fluid interfaces (33-35). The understanding of the adsorption kinetics of stearic acid at fluid interfaces is important for the description of its dynamic surface properties. This is not only an interesting subject in basic research, but also very important for fabricating stable, homogeneous and ordered molecular films.

Further, we examine the diffusion approach, its simplifying assumptions, and Langmuir adsorption kinetics for the adsorption of stearic acid at the oil/water interface. As a first step, we apply the theory of diffusion controlled kinetics on ideal interfacial layers and the Langmuir adsorption kinetics to experimental data of the adsorption of stearic acid at the oil/water interface.

Furthermore, we extend the diffusion theory for non-ideal adsorbed layers at liquid/liquid interfaces (24) and we develop a theoretical approach based on the Ward and Tordai's diffusion equation associated with a two dimensional state equation of van der Waals type and a new diffusion equation is derived and used to describe the dynamic interfacial pressures.

This approach is developed and an analytical procedure of calculation is proposed to solve the resulting new diffusion controlled equations for the surfactant adsorption at liquid/liquid interfaces.

Finally, a mathematical procedure is formulated to determine the diffusion coefficient, the subsurface concentration and the molecular interaction parameters within the adsorbed layers of surfactant at liquid/liquid interface.

Theoretical Models of Adsorption Kinetics

Diffusion Controlled Kinetic Model

Diffusion controlled adsorption was analyzed quantitatively by Ward and Tordai (5, 24) using the following equation:

$$\Gamma(t) = 2\left(\frac{D}{\pi}\right)^{1/2}\left\{c_0 t^{1/2} - \int_0^{t^{1/2}} c_s(t-\tau)d\tau^{1/2}\right\} \quad [1]$$

where $\Gamma(t)$ is the dynamic adsorption of the surfactant from an infinite bulk phase at the interface up to the time t, *i.e.*, $\Gamma(t)$ is the amount of the solute which has diffused across the subsurface into the interface, up to the time t; D stands for the bulk diffusion coefficient of the surfactant (defined by Fick's equation); π is 3.1415; c_0 is the surfactant bulk concentration far from the surface; $c_s(t)$ is the subsurface concentration and τ stands for a dummy variable ranging from 0 to t. At zero time, $c_s(t) = 0$. Later, it begins to increase and $c_s(t)$ becomes equal to c_0, when the adsorption equilibrium is attained.

In Eq. [1] the second term on the right side contains the back diffusion integral taking into account the desorption process. Practically, at the beginning this integral vanishes and the second term may be neglected, obtaining the short time approximation:

$$\Gamma(t) = 2\left(\frac{D}{\pi}\right)^{1/2} \cdot c_0 t^{1/2} \quad [2]$$

Another approximation has been derived for long time by presuming that at long time $c_s(t)$ is almost constant. In this approach one obtains:

$$\Gamma(t) = 2(c_0 - c_s(t))\left(\frac{D}{\pi}\right)^{1/2} t^{1/2} \quad [3]$$

Both Eqs. [2] and [3] suggest a proportionality of the adsorption with $t^{1/2}$. Generally, the dynamic interfacial tension, σ(t), or the dynamic interfacial pressure, Π(t), is measured and used as a tool to investigate the surfactant adsorption at the fluid interfaces.

In order to establish a correlation between the adsorption Γ(t) and the dynamic interfacial tension σ(t) or the dynamic interfacial pressure Π(t) = σ_o – σ(t), frequently, the surface state equation:

$$\Pi(t)\ A(t) = kT \quad \text{or} \quad \Pi(t) = \Gamma(t)kT \qquad [4]$$

is used, which is the two dimensional analog of the perfect gas state equation (22, 27); σ_0 represents the interfacial tension of the pure interface in the absence of the surfactant. It is argued that the state equations apply whether the monolayer is in equilibrium with the subsurface or whether it is not.

Combining Eq. [4] with Eqs. [2] and [3], respectively, one obtains:

$$\Pi(t) = 2kT\left(\frac{D}{\pi}\right)^{1/2} c_0 t^{1/2} \qquad [5]$$

$$\Pi(t) = 2kT\left(\frac{D}{\pi}\right)^{1/2} (c_0 - c_s(t))t^{1/2} \qquad [6]$$

Both Eqs. [5] and [6] show a linear relationship between the dynamic interfacial pressure, Π(t), and $t^{1/2}$. Details on this approach will be presented further on in this investigation.

Langmuir Kinetic Model

On the other hand, by presuming that the molecular diffusion is very fast and the transfer from the subsurface to the surface is the rate limiting step and it follows a *Langmuir kinetics* (6-9), one obtains:

$$y = \ln \frac{\Delta\sigma_0}{\Delta\sigma} = \ln \frac{\sigma_0 - \sigma_e}{\sigma(t) - \sigma_e} = K\,t \qquad [7]$$

where σ(t) stands for the actual and σ_e for the equilibrium interfacial tension and σ_0 for the interfacial tension in the absence of the surfactant. Further, the rate constant K is given by:

$$K = \frac{k_1}{\Gamma_\infty} c_0 + \frac{k_2}{\Gamma_\infty} \qquad [8]$$

where k_1 is the rate constant of adsorption (cm s^{-1}), k_2 stands for the rate constant of desorption (mole cm^{-2} s^{-1}) and Γ_∞ is the maximum adsorption (mole cm^{-2}) at the saturation of the liquid/liquid interface with surfactant molecules.

In the present paper the dynamic interfacial pressures, $\Pi(t) = \sigma_o - \sigma(t)$, at the benzene/water interface have been measured for benzene solutions of stearic acid (octadecanoic acid: SA) of various SA concentrations. The validity of the above equations has been tested and an attempt is made to derive a new equation for the diffusion controlled adsorption, taking into account the non-ideal behavior of adsorbed films at liquid interfaces, particularly for high bulk surfactant concentrations. The results of the analysis of the experimental data performed on the basis of the new equation shows that the latter allows a better description of the adsorption kinetics, than the other equations given above.

Experimental

Stearic acid (octadecanoic acid: SA) was a synthetic commercial product of high purity (minimum 99%) purchased from Sigma. Benzene pro-analysis was purchased from Merck. All chemicals were used without an additional purification. Twice-distilled water of pH 2 was used, containing 0.01 mole/dm^3 of hydrochloric acid, as the aqueous phase. Volumetric aqueous solutions of HCl pro-analysis were purchased from Reactivul Bucharest.

Stearic acid at pH 2 forms uncharged adsorbed monolayer, the molecules being completely unionized (29). Due to the very low solubility of stearic acid in water of pH 2, any transport across the benzene/water interface can be neglected. The pH of the aqueous solutions was constant during all experiments and it was measured by an MV-84 type pH-meter by using a glass electrode.

Dynamic surface tensions in the time range from 1 minute up to 120 minutes were measured by pendant drop and by ring method for pure benzene and benzene solutions of various stearic acid concentrations at the interface with aqueous solutions of pH 2.

The pendant drop technique was described by us elsewhere (23). The shape of drops was recorded on a highly quality film in order to determine the characteristic drop diameters. By using an appropriate computer program the dynamic interfacial tension values were finally determined.

Experimental data obtained by the pendant drop technique were compared with the data obtained by ring method described by us previously (36). The agreement between the two methods is excellent and the deviations

do not exceed the error of the individual method. The accuracy of interfacial tension measurements was ± 0.1 mN/m, in agreement with literature data (20, 37). All measurements were performed at constant temperature of 20 ± 0.1 ^{o}C.

Results and Discussions

Dynamic interfacial tension σ(t) values obtained by means of the pendant drop method, allowed us to calculate the corresponding Π(t) = σ_0 – σ(t) interfacial pressure values. The Π(t) *versus* time (t) curves, characterizing the adsorption process of SA from benzene at the benzene/water (pH 2) interface is presented in Fig.1.

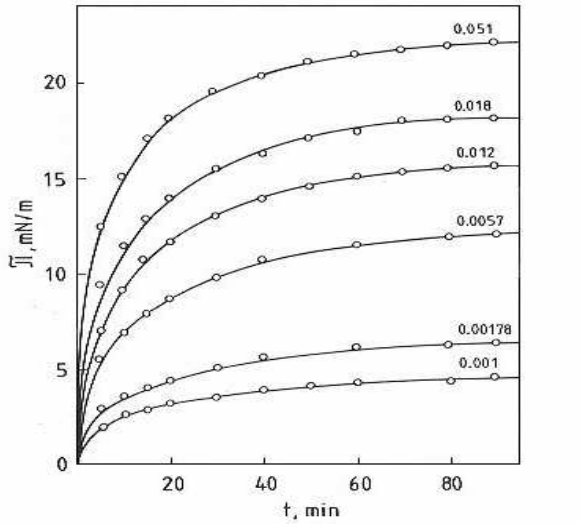

Fig. 1.
Experimental dynamic interfacial pressures, Π(t) = σ_o – σ(t) in mN/m, of stearic acid (SA) benzene solutions as function of time, t in min, at the benzene/water of pH 2 interface. Figures indicate the bulk concentration C_0 of stearic acid in benzene, in mole dm^{-3}. Solid lines calculated by Eq. [18].

As can be seen, the interfacial pressures vary with surfactant bulk concentrations and with time over a wide range of time, from 0 to 90 min. Generally, the equilibrium interfacial pressures (Π_e in mN/m) are recorded at 120 min when the adsorption equilibrium is completely attained and it is demonstrated by the constant value of the interfacial pressures.

The validity of Eq. [7] has been tested by calculating the left hand side (denoted y) of this equation, by using the σ(t) and σ_e values (the latter ones being measured at 120 min) and the interfacial tension of the pure benzene/

water interface in the absence of surfactant was taken σ_o = 34.7 mN/m.

Inspecting the experimental data, it is found that y *versus* t data exhibit a quite good linearity, although the straight lines do not pass through the origin of the coordinate system, *i.e.* actually instead of Eq. [7] one has:

$$y = \ln \frac{\sigma_0 - \sigma_e}{\sigma - \sigma_e} = B + K t \qquad [7']$$

By performing a linear regression, the parameters B and K have been determined. Results are presented, together with the correlation coefficients, *r*, in Table I. In the last column *n* indicates the number of experimental points used in the linear regression.

Table I.
The B and K parameters of Eq. [7'].

C_0 mole dm^{-3}	B	K min^{-1}	r	n
0.001	0.430	0.0397	0.9991	7
0.00178	0.374	0.0396	0.9977	7
0.0057	0.395	0.0406	0.9990	8
0.012	0.439	0.0415	0.9978	8
0.018	0.568	0.0431	0.9994	9
0.051	0.566	0.0501	0.9949	10

As seen from Table I, the B values are rather far from zero. This means that the basic hypothesis used to derive Eq. [7] is not perfectly valid, presumably the diffusion equilibrium is not yet established, and consequently the boundary condition $c_s(t) = c_0$ is not fulfilled. Nevertheless, from the K values reported in Table I, some conclusions can be drawn. As seen, with increasing c_0 the K values derived also increase, as expected on the basis of Eq. [8] and the dependence of K with c_0 exhibits indeed a quite good linearity. The relative adsorption k_1/Γ_∞ and desorption k_2/Γ_∞ rate constants derived by means of linear regression Eq. (8) and the corresponding correlation coefficients are presented in Table II.

Table II.
Relative adsorption, k_1/Γ_∞, and desorption, k_2/Γ_∞, rate constants derived by Eq. [8] from K values listed in Table I.

Surfactant	k_1/Γ_∞ mole $^{-1}$ dm^3 min $^{-1}$	k_2/Γ_∞ min $^{-1}$	r	k_1/k_2 mole $^{-1}$ dm^3
Stearic acid	0.212	0.0392	0.9990	5.4
Dibucaine	7.25	0.159	0.9914	45.6
Tetracaine	4.99	0.149	0.9988	33.5

Table II contains also the same magnitudes previously obtained for two anesthetics, *viz*. dibucaine and tetracaine, under similar working conditions (24).

The analysis of data in Table II shows the quite good validity of Eq. [8], reflected by the correlation coefficient values. The relative rate constant values are rather reasonable and their k_1/k_2 ratios are in substantial agreement with published data (6-8) for the adsorption of various surfactants at liquid/liquid interfaces. These ratios represent the equilibrium adsorption constants and characterize the interfacial activity of these biocompounds at the oil/water interface. In this respect, the k_1/k_2 value for dibucaine is higher than the corresponding value for tetracaine suggesting a higher interfacial activity of the dibucaine in agreement with the interfacial pressure measurements at the oil/water interface.

Generally, the relative rate constant values (Table 2) for anesthetics are much higher than those corresponding to stearic acid. These values are not easy to compare because the mechanism of adsorption and desorption of these two types of biocompounds (i.e. anesthetics and fatty acids) is completely different and consequently the rate constants are determined by different factors. In spite of the different mechanism for adsorption, both fatty acid and anesthetics strongly adsorb at the oil/water interface and show a certain type of similarity in their adsorption behavior.

In the case of stearic acid, molecules adsorb from oil phase to the oil/water interface immersing their unionized polar groups into the water phase. The driving force for the adsorption of stearic acid molecules is the change in enthalpy due to the hydration of their adsorbed hydrophilic groups, when they immerse into the water phase being accompanied by conformational rearrangements in the hydrocarbon chains. Unlike stearic acid, anesthetics are ionized water soluble compounds. They adsorb from water to the oil/water interface by penetrating their hydrophobic chains into

the oil phase. Their adsorption is controlled by the hydrophobic effect, by the electrostatic interactions among the ionized polar groups, and by the hydrophobic interactions among the hydrophobic chains and the oil phase. According to the hydrophobic effect, the hydrocarbon chains in water phase are surrounded with structured water. Therefore, the adsorption of anesthetics is also accompanied by the increase of the entropy of the system because of the destruction of the ordered structure of water molecules formed around the hydrophobic chains in aqueous phase.

Although these results seem to be reasonable, the quite high B values reported in Table I show that Eq. [7], successfully used to describe the adsorption at the air/water interface (6-8), in our case is an approximation and the diffusion might play an important part in the overall adsorption process. Consequently, we further test the validity of Eqs. [5] and [6].

For this purpose, the experimental Π(t) values calculated from σ_0 and σ(t) values are presented *versus* $t^{1/2}$ in Fig. 2.

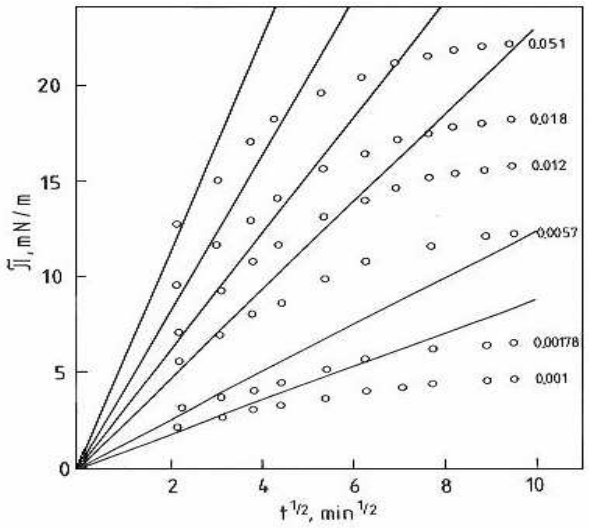

Fig. 2.
Experimental dynamic interfacial pressures of stearic acid benzene solutions at the interface with water of pH 2 as function of $t^{1/2}$. (Symbols as in Fig. 1).

If the Eq. [5] or Eq. [6] was valid, the Π(t) *versus* $t^{1/2}$ curves would exhibit a linear portion at least at small t values. This is why the tangencies to the experimental curves for t = 0 were constructed (Fig. 2). Although, the experimental curves exhibit an important negative deviation from these straight lines, certain linearity may be observed. In order to obtain a clear

image, a linear regression analysis has been performed by adding successively the experimental data, one by one, and by calculating every time the parameters of the following equation:

$$\Pi(t) = mt^{1/2} + p \qquad [9]$$

The general picture is the following, by adding the experimental data in the order of increasing t values, the slope of the straight line (*i.e.,* the m value) diminishes, and the ordinate intercept p increases. In the same time the correlation coefficient diminishes.

Results are presented in Table III, where the limits of m and p values are given. Those obtained by means of the first three experimental points (noted m_i and p_i, respectively), as well as the values obtained with a final number, n_f, of experimental points (noted m_f and p_f, respectively), for which one had still $r > 0.99$, r being the correlation coefficient. In Table III are also listed the total number, n_{max}, of the experimental points obtained for every bulk concentration of SA.

Being more specific, Eq. [9] is a general form of Eqs [5] and [6].

Table III.
Limits of the m (m_i and m_f) and p (p_i and p_f) parameters of Eq. [9] for $r > 0.99$. For symbols see the text.

C_0 mole dm^{-3}	m_i mN m^{-1} $min^{-1/2}$	m_f mN m^{-1} $min^{-1/2}$	p_i mN m^{-1}	p_f mN m^{-1}	n_f	n_{max}
0.001	0.47	0.33	1.16	1.59	10	10
0.00178	0.63	0.48	1.59	1.72	7	9
0.0057	1.47	1.26	2.23	2.85	6	9
0.012	2.27	2.08	1.96	2.48	4	11
0.018	2.14	1.88	4.64	5.92	5	11
0.051	2.68	2.50	6.57	7.06	4	11

The analysis, of the data given in Table III, shows that Eqs. [5] and [6] are very rough approximations, because p from Eq. (9) is very far from the expected zero value, especially in the case of higher SA concentrations. Further, the decrease of the m values with increasing time ($m_i > m_f$) indicates negative deviations from the linearity predicted by Eq. [5] or Eq. [6], both being consistent with the case of diffusion adsorption for the ideal

behavior, given by Eq. (4), of the interfacial film of adsorbed surfactant.

As a first approximation let us presume that at low t values Eq. [5] is valid and consequently in Eq. [9] one has p = 0 and m_i, the coefficient of $t^{1/2}$, is given by the following equation:

$$m_i = 2kT\left(\frac{D}{\pi}\right)^{1/2} c_0$$

By expressing D, one obtains:

$$D = \frac{\pi m_i^2}{(2kTc_0)^2} \qquad [10]$$

We mention that in Eq. [1] c_0 means the bulk concentration expressed in surfactant molecules/volume. Consequently, if one gives m_i in dyne cm^{-1} $s^{-1/2}$ (see Table IV), k in erg/(molecule grade) and c_0 in molecules cm^{-3}, D will be obtained in cm^2 s^{-1}. Obviously, if the bulk concentration is given as C_0 mole/L, one has $c_0 = 10^{-3}$ N_A C_0, where N_A stands for Avogadro's constant. Diffusion coefficients, D values, calculated by means of Eq. [10] from m_i values, listed in Table III, are given in Table IV.

Table IV.
Diffusion coefficients, D and D_0 calculated by Eq. [10], and C_s values calculated by Eq.[12] from the slopes m_i taken from Table III.

C_0 mole dm^{-3}	m_i dyne cm^{-1} $s^{-1/2}$	D 10^{11} cm^2 s^{-1}	D_0 cm^2 s^{-1}	C_s 10^3 mole dm^{-3}
0.001	0.0607	0.492		0
0.00178	0.0813	0.278		0.44
0.0057	0.1900	0.148	$4.92\ 10^{-12}$	2.57
0.012	0.2930	0.0796		7.17
0.018	0.2760	0.0314		13.4
0.051	0.3460	0.00614		45.3

As seen, in Table IV, D diminishes with increasing bulk concentration, suggesting the idea that Eq. [6] might be a better approach than Eq. [5]. One may take, then, from Eq. [6] for m_i the following expression:

$$m_i = 2kT\left(\frac{D}{\pi}\right)^{1/2}(c_0 - c_s) \qquad [11]$$

It is reasonable to presume that the subsurface concentration C_s (expressed in mole/L) increases with increasing bulk concentration C_0. Let us presume as a first approach that $C_s = 0$ for $C_0 = 0.001$ mole/L. In this case a D_0 value can be obtained by means of Eq. [10]. Further, by using this D_0 value and Eq. [11], C_s values may be derived, from the m_i slopes obtained for higher concentrations, *viz*., by means of the following relation:

$$C_s = C_0 - \frac{\pi^{1/2} m_i}{2kT \cdot 10^{-3} N_A D_0^{1/2}} \qquad [12]$$

The values of subsurface concentrations (C_s, calculated by Eq.[12]) and diffusion coefficient D_0 are also given in Table IV.

As seen, C_s increases with increasing C_0, as one might expect. However, the diffusion coefficient is with several orders of magnitude less than real ones ($D = 5\ 10^{-6}$ cm^2 s^{-1}) assumed for surfactants diffusing through aqueous phase to the air/water interface (7). This means, that Eqs. [5] and [6] are extremely rough approximations to fit these experimental data.

The remarkable low values of the diffusion coefficients are probably due to a slow orientation (7, 38) of the polar head groups of SA molecules at the interface and to a slow conformational transition in the long hydrocarbon chains of SA molecules to finally achieve their correct orientation at the adsorption equilibrium. These effects can also explain the slow interfacial pressure increase to reach its equilibrium value. As an alternative, the long time dependence of the interfacial pressure can be attributed to the interactions among SA molecules at the oil/water interface, where these SA molecules relax and reorient leading to their proper molecular arrangement characteristic for the adsorption equilibrium.

Modeling of the New Diffusion Kinetic Equation

Eqs. [5-6] and [9-12] have been obtained by presuming the state equation [4] to be valid. But interfacial monolayers obey Eq. [4] only at very small Π values, practically for $\Pi \rightarrow 0$. One of the best state equations, proposed for non-ionic monolayers (39) and quoted and used by others (40-42), is of the following shape:

$$\left(\Pi + \frac{\alpha}{A^{3/2}}\right)(A - A_0) = kT \qquad [13]$$

where A stands for the mean molecular area, A_0 for the own molecular area of the surfactant and α is an interaction parameter. Eq. [13] was found to describe very well the compression isotherm of miscellaneous monolayers (40, 41), especially if the interaction parameter α and the own molecular area A_0 are treated as adjustable parameters.

From state equation [13], Π may be expressed as:

$$\Pi = \frac{kT}{A - A_0} - \frac{\alpha}{A^{3/2}} = \frac{kT\Gamma}{1 - \Gamma A_0} - \alpha\Gamma^{3/2} \qquad [14]$$

Let us denote:

$$x = 2(c_0 - c_s)\left(\frac{D}{\pi}\right)^{1/2} \qquad [15]$$

Thus, the long time approximation of diffusion, given by Eq. [3], may be written as $\Gamma(t) = xt^{1/2}$. Then, combining Eqs. [3], [13] and [15], one obtains:

$$\Pi = \frac{kTxt^{1/2}}{1 - A_0 xt^{1/2}} - \alpha x^{3/2} t^{3/4} = kTx\left[\frac{t^{1/2}}{1 - A_0 xt^{1/2}} - \frac{\alpha x^{1/2}}{kT} t^{3/4}\right] \qquad [16]$$

Therefore, one may expect Eq. [16] to describe better the time dependence of Π, than Eq. [6] does.

Introduction of Dimensionless Variables

In order to study the properties and possibilities of Eq. [16], let us introduce a reduced time scale. If in an experiment Π has been followed from t = 0 up to a maximum time t_m, a reduced time (noted τ) can be defined as:

$$\tau = \frac{t}{t_m} \qquad [17]$$

Combining Eqs. [16] and [17] one obtains:

$$\Pi = kTxt_m^{1/2}\left[\frac{\tau^{1/2}}{1 - A_0 xt_m^{1/2}\tau^{1/2}} - \frac{\alpha x^{1/2}}{kT} t_m^{1/4}\tau^{3/4}\right]$$

The Eq. [17] may be written as:

$$\Pi = a\left[\frac{\tau^{1/2}}{1-b\tau^{1/2}} - c\tau^{3/4}\right] = a\varphi(\tau) \qquad [18]$$

with:

$$a = 2kT(c_0 - c_s)\left(\frac{Dt_m}{\pi}\right)^{1/2}$$

$$b = 2A_0(c_0 - c_s)\left(\frac{Dt_m}{\pi}\right)^{1/2}$$

$$c = \frac{2^{1/2}\alpha(c_0 - c_s)^{1/2}}{kT}\left(\frac{Dt_m}{\pi}\right)^{1/4}$$

From the expression of the parameters *a, b* and *c* one obtains:

$$D = \left[\frac{a}{2kT(c_0 - c_s)}\right]^2 \frac{\pi}{t_m}; \quad A_0 = \frac{kTb}{a}; \quad \alpha = \frac{c}{a^{1/2}}(kT)^{3/2} \qquad [19]$$

Obviously, if $t = t_m$, from Eq. [17] one has $\tau = 1$ and Eq. [18] becomes:

$$\Pi_m = a\varphi(1) = a\left[\frac{1}{1-b} - c\right] \qquad [20]$$

Let us introduce also for the interfacial pressure a reduced scale:

$$\Pi^* = \frac{\Pi}{\Pi_m}$$

where Π_m stands for the maximum interfacial pressure, corresponding to $t = t_m$. By using the Eqs. [18] and [20], this reduced interfacial pressure is expressed as:

$$\Pi^* = \frac{\Pi}{\Pi_m} = \frac{\varphi(\tau)}{\varphi(1)} \qquad [21]$$

Thus one obtains finally for the time dependence of the interfacial pressure:

$$\Pi = \frac{\Pi_m}{\varphi(1)}\varphi(\tau) \qquad [22]$$

By comparing Eq. [22] with Eq. [18] it is obvious that:

$$a = \frac{\Pi_m}{\varphi(1)} \qquad [23]$$

Procedure of Calculations

In order to test the utility of Eq. [22] or of Eq. [18], we studied the influence of the parameters *b* and *c* upon the shape of the Π/a *versus* τ and Π^* *versus* τ curves. For this purpose theoretic curves have been constructed. Some examples are given in Figs. 3-6.

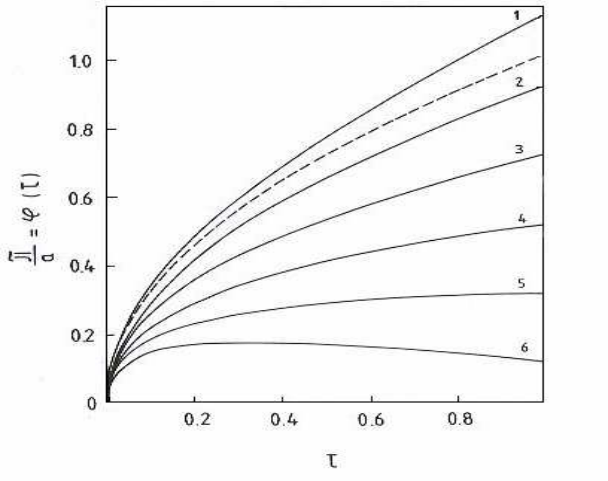

Fig. 3.

Influence of the *c* parameter upon the theoretical $\varphi(\tau)$ *versus* τ curves, given by Eq. [18], for *b* = 0.1. The *c* values: curve (1) 0; (2) 0.2; (3) 0.4; (4) 0.6; (5) 0.8; (6) 1.0. Dashed line curve: *b* = *c* = 0.

In Fig. 3 the influence of the *c* parameter, upon the shape of the Π/*a* = $\varphi(\tau)$ *versus* the dimensionless τ curves, is illustrated by taking the constant *b* = 0.1 value. Fig. 4 illustrates the influence of the *b* parameter for the constant *c* = 0.6 value.

Since parameters *b* and *c* influence also the $\varphi(1)$ value (see Eq. [20]), the shift of the calculated curves makes their comparison rather difficult. The influence of these parameters is more clear if the $\Pi^* = \varphi(\tau)/\varphi(1)$ *versus* τ curves are constructed. These are shown in Figs. 5 and 6.

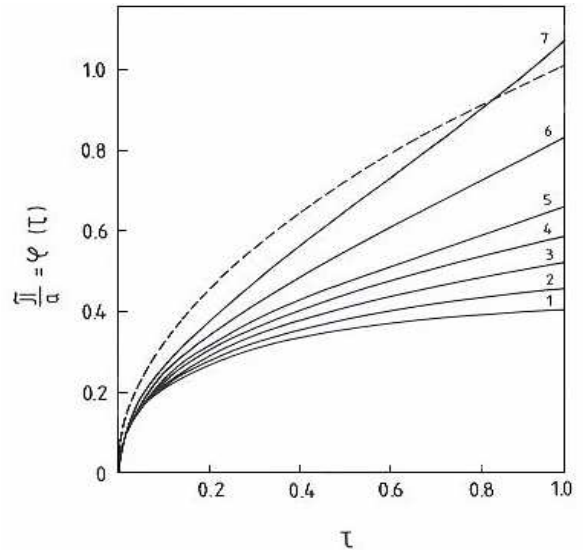

Fig. 4.

Influence of the *b* parameter upon the theoretical φ(τ) *versus* τ curves, given by Eq. [18], for *c* = 0.6. The *b* values: curve (1) 0; (2) 0.05; (3) 0.1; (4) 0.15; (5) 0.2; (6) 0.3; (7) 0.4. Dashed line curve: *b* = *c* = 0.

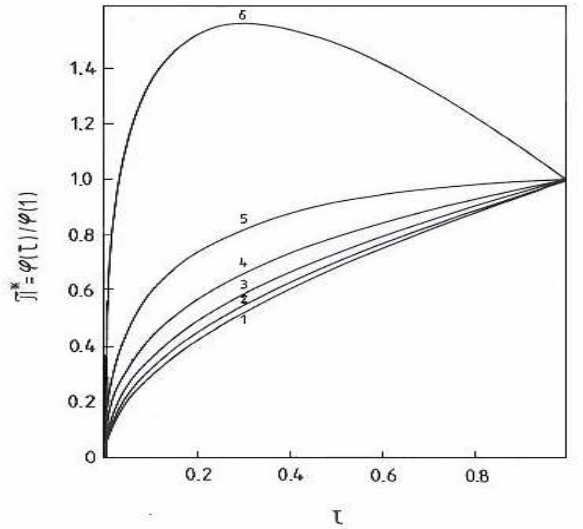

Fig. 5.

Influence of the *c* parameter upon the theoretical Π^* *versus* τ curves, given by Eq. [21]. The *b* and c values as in Fig. 3.

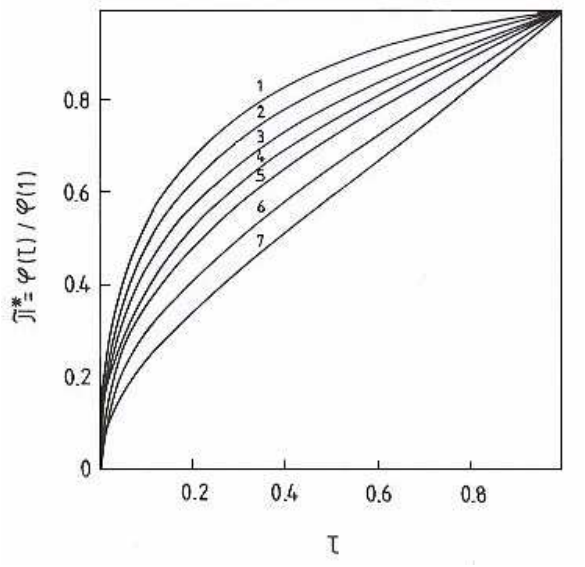

Fig. 6.
Influence of the *b* parameter upon the theoretical Π^* *versus* τ curves, given by Eq. [21]. The *b* and *c* values as in Fig. 4.

It is worth mentioning that for $b = 0.1$ and $c = 1.0$ both $\varphi(\tau)$ (curve 6 in Fig. 3) and Π^* (curve 6 in Fig. 5) exhibit a maximum for about $\tau = 0.3$. This would imply the appearance of a maximum interfacial pressure at a certain time, followed by the diminution of Π. This is of course unrealistic. Therefore, it is obvious that not all *b* and *c* pairs can describe the real adsorption kinetics. Further, the curve for $b = 0.4$, $c = 0.6$ (curve 7 in Fig. 4) indicates the adsorption rate to decrease down to a minimum value, followed by the acceleration of the adsorption. This also cannot happen in a real adsorption process, since the more occupied the adsorption sites, the less will be the adsorption rate, becoming zero at the adsorption equilibrium.

Although, not all calculated $\varphi(\tau)$ functions correspond to real adsorption behavior of surfactants, the main feature is that in the case of *diffusion controlled adsorption* the own molecular area A_0 and the intermolecular interactions expressed by the parameter α may count for both positive and negative deviations from the $t^{1/2}$ law (see Fig. 2).

Since according to the $t^{1/2}$ law expressed by Eq. [6] one has $\Pi^* = \tau^{1/2}$, the deviation of the reduced surface pressure from the $t^{1/2}$ law may be expressed by the function:

$$\Delta = \frac{\varphi(\tau)}{\varphi(1)} - \tau^{1/2} \qquad [24]$$

The influence of the *c* and *b* parameters upon the theoretical Δ vs. τ curves is illustrated in Figs. 7 and 8, respectively. It is obvious that both positive and negative Δ values may appear and the deviation from the $t^{1/2}$ law may be very important.

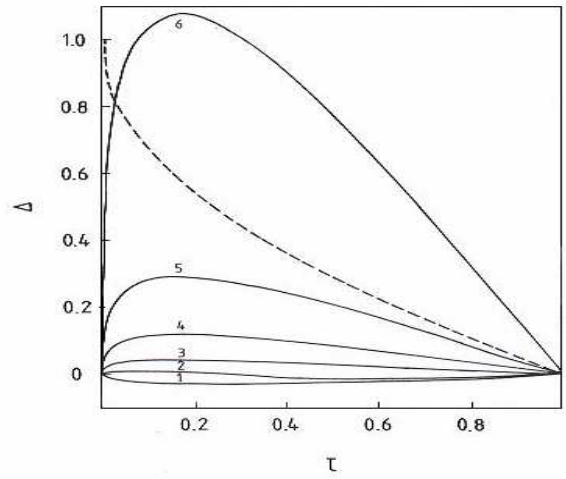

Fig. 7.
Influence of the *c* parameter upon the theoretical Δ *versus* τ curves, given by Eq. [24].The *b* and *c* parameters as in Fig. 3.

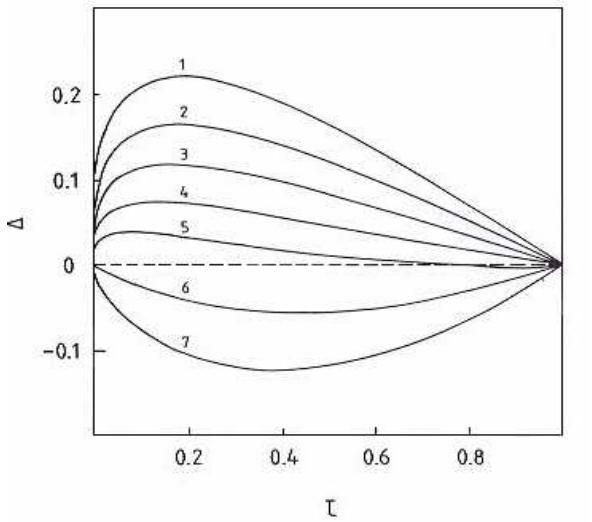

Fig. 8.
Influence of the *b* parameter upon the theoretical Δ *versus* τ curves, given by Eq. [24]. The *b* and *c* parameters as in Fig. 4.

In real systems, as seen in Fig. 2, with increasing time negative deviations from the $t^{1/2}$ law appear. In a Π^* vs. τ plot this means that the curve is more convex (has a higher curvature) as compared to $\tau^{1/2}$, i.e. Δ has positive values. Consequently, negative Δ values indicate unrealistic theoretical curves. Even the positive values have an upper limit, it is easy to see that the Π vs. t curve passes through a maximum if $\Delta > 1 - \tau^{1/2}$. The dashed line curve in Fig. 7 indicates this upper limit $\Delta = 1 - \tau^{1/2}$.

Since the Δ vs. τ curves exhibit important shifts if *b* or *c* is modified, in order to illustrate the influence of the parameters b and c upon the shape of the curves, we choose a set of *b* – *c* pairs which oblige the Δ vs. τ curves to pass through a common point. If we impose the condition that at a certain τ_0 value the Δ function must be equal to Δ_0, Eq. [24] becomes:

$$\Delta_o = \frac{\varphi(\tau_0)}{\varphi(1)} - \varphi_0^{1/2}$$

From this relation one might express the *c* parameter and one obtains:

$$c = \frac{1}{\Delta_0 + \tau_0^{1/2} - \tau_0^{3/4}} \left[\frac{(\tau_0^{1/2} - \tau_0)b}{(1-b)(1-\tau_0^{1/2}b)} + \frac{\Delta}{1-b} \right] \qquad [25]$$

Table V.
The *b* and *c* pairs, calculated by Eq. [26], ensuring $\Delta = 0.2$ for $\tau = 0.2$.

No.	b	c
1	0	0.575
2	0.02	0.601
3	0.05	0.643
4	0.10	0.721
5	0.15	0.810
6	0.20	0.913
7	0.25	1.033
8	0.30	1.172
9	0.35	1.337
10	0.40	1.534

Eq. [25] allows us to calculate for a given Δ_0 - τ_0 pair the *c* parameter as function of *b*. Thus, for $\Delta_0 = \tau_0 = 0.2$ one obtains:

$$c = \frac{0.71b}{(1-b)(1-0.447b)} + \frac{0.574}{1-b} \qquad [26]$$

Some illustrative examples of *c* – *b* pairs ensuring $\Delta = 0.2$ for $\tau = 0.2$, calculated by means of Eq. [26] are given in Table V.

For cases 1, 3, 4, 6, 7 and 8 whole Δ vs. τ curves are given in Fig. 9.

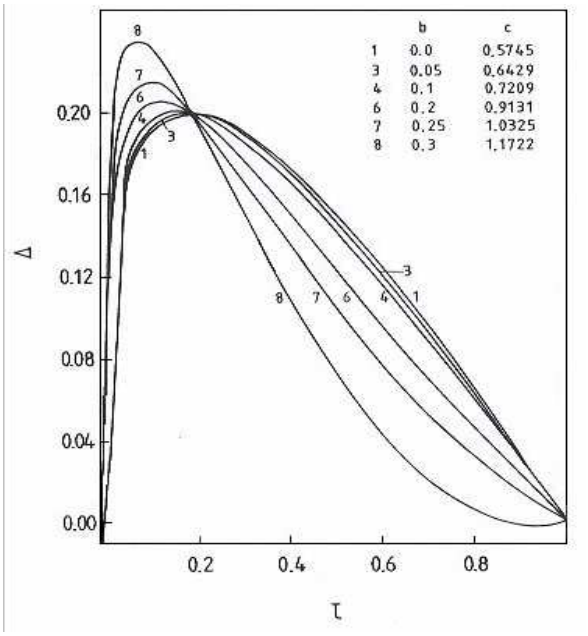

Fig. 9.
Some Δ *versus* τ curves passing through the point $\Delta = \tau = 0.2$. Figures indicate the *b* and *c* pairs given in Tab. 5.

It is clear that Eq. [18] corresponds to a very flexible function able to describe well a great variety of curves. Since for *b* = 0.3 the deviation Δ arrives in the negative region for $\tau > 0.85$, Eq. [26] may give *b* – *c* pairs corresponding to real experimental curves only if *b* < 0.3.

Deriving of the Parameters of Eq. [18] from Experimental Data

In order to derive the parameters *a, b* and *c* of Eq. [18] we adopted the following procedure of working up the experimental data given in Fig. 1. We have chosen t_m = 90 min and calculated for each experimental point the reduced parameters τ and Π^*. Further we calculated, for the found τ values, the theoretical Π^* values by taking certain *b – c* pairs. In the first approach we took *b* = 0 and calculated theoretical Π^* values for different *c* ones. In the case of each *c* value the standard deviation (SD) of the experimental Π^* values from the theoretical ones was calculated. By means of a systematic variation of *c* the minimum standard deviation $(SD)_m$ was sought for. Then, the calculations were repeated for other *b* values, too. Thus, a double minimization of the standard deviation has been performed and the *b – c* pair ensuring the least value for the standard deviation has been taken for the most realistic parameter values.

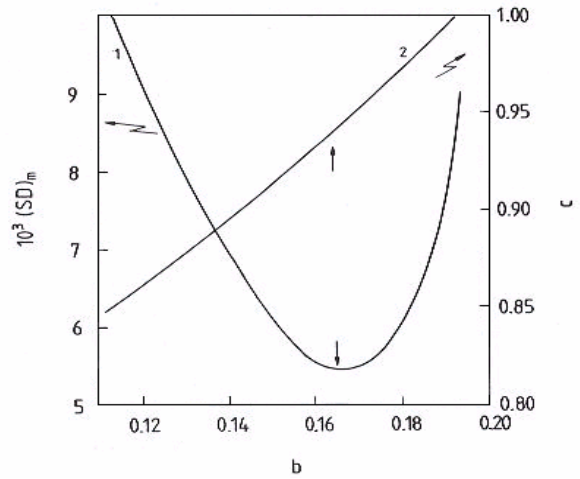

Fig. 10.
Deriving of *b* and *c* parameters for the stearic acid benzene solution of C_0 = 0.051 mole dm^{-3} at the interface with water phase of pH 2.

This calculation procedure is visualized in Fig. 10 for the stearic acid oil solution of 0.051 mole/L. Curve 1 gives the minimum standard deviation $(SD)_m$ obtained for different b values presumed and curve 2 indicates the corresponding *c* value. Let us take, e.g. *b* = 0.12. Eq. [21] allows us to calculate theoretical Π^* values corresponding to *b* = 0.12 and to different *c* values. In each case, i.e. with each *c* value presumed, the standard deviation:

$$SD = \sqrt{\frac{1}{n}\sum\left(\Pi_t^* - \Pi_e^*\right)^2} \qquad [27]$$

is calculated where n stands for the number of points used, and Π_t^* and Π_e^* stand for the theoretical and for the experimental reduced interfacial pressure, respectively. By trying different *c* values, one observed that the standard deviation will be the less for *c* = 0.86, viz. it will be equal to $(SD)_m$ = 0.00928. Thus, we obtained a point on curve 1 and a point on curve 2.

By repeating these calculations for other *b* values, eventually one obtains the whole curve 1 and curve 2. As seen, curve 1 has a minimum (indicated by a downward vertical arrow), corresponding to *b* = 0.163, this minimum $(SD)_m$ is ensured by a *c* value equal to 0.937 (indicated on the curve 2 by an upward vertical arrow).

By using the *b* and *c* values obtained, φ(1) may be easily calculated according to Eq. [20], as well as the corresponding parameter *a* by means of Eq. [23]. Results obtained by means of this procedure are presented in Table VI.

Table VI.
Parameters of Eq. [18] derived from the experimental dynamic interfacial pressures for SA at the benzene/water of pH 2 interface.

C_0 mole dm^{-3}	t_m min	Π_m mN m^{-1}	φ(1)	a	b	c	$(SD)_m$ mN m^{-1}
0.001	90	4.5	0.3820	11.78	0.0813	0.706	0.0060
0.00178	90	6.4	0.4096	15.62	0	0.590	0.0046
0.0057	90	12.1	0.3682	32.86	0.0039	0.635	0.0019
0.012	90	15.6	0.3506	44.50	0	0.649	0.0019
0.018	90	18.1	0.3367	53.76	0.0019	0.665	0.0022
0.051	90	22.0	0.2575	85.43	0.163	0.937	0.0054

The parameter values given in Table VI allow us to construct by means of Eq. [18] theoretical Π vs. t curves. These curves are given in Fig. 1 as full line curves. Thus, it is demonstrated that Eq. [18] describes very well the experimental Π vs. t data within the experimental errors.

Inspection of Table VI shows that the *a* parameter increases with increasing bulk concentration C_0 of stearic acid. The *c* parameter shows

also a clear increasing tendency. The *b* parameter has very small values frequently vanishing ones and cannot be correlated with C_0.

With respect to the meaning of the parameter *a*, according to Eq. [19] it allows us to calculate the diffusion coefficient D. Let us assume as a first approach that $C_s = 0$ at all bulk concentrations C_0. By taking into account that $c_0 = C_0\ 10^{-3}\ N_A$, Eq. [19] becomes:

$$D = \left(\frac{a}{2kT \cdot 10^{-3} \cdot N_A \cdot C_0} \right)^2 \frac{\pi}{t_m} \qquad [28]$$

Diffusion coefficients calculated by means of Eq. [28], and by using the *a* values listed in Table VI, are presented in Table VII.

Table VII.

Diffusion coefficients, D and D_0, calculated by Eq. [28], subsurface concentrations C_s, calculated by Eq. [29], and interaction parameters α calculated by Eq. [19], from the a and c parameters of Eq. [18]. Symbols are defined in the text.

C_0 mole dm^{-3}	D 10^{10} cm^2 s^{-1}	D_0 10^{10} cm^2 s^{-1}	C_s 10^3 mole dm^{-3}	α 10^{22} dyne cm^2
0.001	0.3430		0	16.7
0.00178	0.1900		0.45	12.1
0.0057	0.0821	0.343	2.91	9.02
0.012	0.0840		8.22	7.92
0.018	0.0220		13.4	7.38
0.051	0.0069		43.7	8.24

By analyzing the D values listed in Table VII and by comparing them with the values given in Table IV, one can see that the general picture is similar, since D values show a decreasing tendency with increasing bulk concentration of stearic acid and seem to be more realistic, their values being higher with about one order of magnitude as compared to the previous approach (Eqs. [5] and [6]).

As a second approach we shall presume that $C_s = 0$ only in the case of the surfactant solution of 0.001 mole/L and it increases with increasing bulk concentration, but the diffusion coefficient remains the same D_0 as obtained from the a value for the 0.001 mole/L solution. In this assumption C_s may be calculated from the expression of D given in Eq. [19] and one obtains:

$$C_s = C_0 - \frac{\pi^{1/2} \cdot a}{2kT \cdot 10^{-3} \cdot N_A \cdot D_0^{1/2} \cdot t_m^{1/2}} \quad [29]$$

The C_s values calculated by Eq. [29] are presented in Table VII and they increase linearly with increasing C_0 as in the case of those C_s values presented in Table IV, but the correlation coefficient is better, r = 0.9994, as compared to r = 0.9983 obtained with C_s values from Table IV. Although the D_0 value (Table VII) is higher with almost one order of magnitude than D_0 value (Table IV), it is far from being realistic. This situation is similar with the adsorption of palmitic acid at the hexane/water interface, for which D = 5.66 10^{-13} cm^2 s^{-1} was reported (5) and the authors consider that the anomalous D value is due to the existence of an activation barrier for the adsorption between the subsurface and the interface.

Generally, the diffusion coefficient obtained for SA is with at least one order of magnitude smaller than its value previously determined for the two anesthetics, e.g. dibucaine and tetracaine (24, 43). This finding is probably related with the structure of anesthetic molecules, since dibucaine and tetracaine have much shorter hydrocarbon chains and are quite rigid molecules, and their diffusion through the bulk phase and penetration into the oil/water interface might occur easier than for stearic acid molecules.

Eq. [19] allows also the calculation of the interaction parameter α from the parameters *a* and *c* of Eq. [18]. The α values are presented also in Table VII. As seen one does not obtain the same value in the case of differing bulk concentrations, viz. a decreasing tendency is observed with increasing C_0. This indicates, similarly to the too low D_0 value, that the process is not purely diffusion controlled and the potential energetic barrier to adsorption (43, 44) and an interfacial reorientation (45-47) of surfactant molecules could play an important part.

By calculating the mean value of the interaction parameter one obtains α = 1.02 10^{-21} dyne cm^2. It is worth mentioning that for stearic acid monolayers spread at the air/water interface we obtained 4.3 10^{-21} dyne cm^2 (42). In the case of the air/water interface in the air phase strong hydrophobic interactions appear between the long hydrocarbon chains, which are almost absent at the benzene/water interface, when the hydrocarbon chains are solvated with benzene molecules hindering the direct interaction between the neighboring SA molecules. Consequently the α value must be much less as compared to the air/water interface. Thus, the above α value seems to be in substantial agreement with our earlier results (42).

The low values of the diffusion coefficients can be further correlated with the presence of an energy barrier of adsorption due to a slow reorientation

(7, 38) of the polar head groups of SA molecules at the interface to finally achieve their proper arrangement or their correct orientation at the adsorption equilibrium. This effect can also explain the slow interfacial pressure increase to reach its equilibrium value.

Therefore, these data represent strong experimental evidence about the non-ideal behavior of adsorbed SA layers at the oil/water interface and about the interfacial reorientation of SA molecules at the oil/water interface, which apparently operates for the adsorption of fatty acids from oil solution to an oil/water interface. It seems that the adsorption of SA from benzene to the benzene/water interface is of this type in agreement with the adsorption of palmitic acid at the hexane/water interface reported earlier (5). Hence, the adsorption process is controlled by the molecular diffusion in the oil phase associated with the surface reorientation and the molecular interactions of stearic acid molecules at the oil/water interface.

Conclusions

A theoretical approach to the dynamic interfacial pressures is developed and a new kinetic Eq. [18] for the diffusion controlled kinetics is proposed, based on Ward and Tordai's diffusion equation associated with a two dimensional van der Waals state equation. This approach is consistent with the case of the non-ideal behavior of the adsorbed films widely used in the kinetic of adsorption of surfactants from concentrated bulk solutions to the liquid interfaces. This provides a possibility for one to determine the diffusion coefficients, subsurface concentrations and intermolecular interaction parameters within adsorbed films of surfactants at the liquid/liquid interfaces. The theory is applied to describe and fit the experimental data of the dynamic interfacial pressures for the adsorption of stearic acid (SA) at the benzene/water interface. Obtained results are in general agreement with similar earlier reported data for the adsorption of palmitic acid (5) and the adsorption of chlorophyll (22) at the different oil/water interfaces.

The adsorption of stearic acid (SA) at the benzene/water interface seems to be a process in which the rate is controlled both by the molecular diffusion from the bulk to the subsurface and by the molecular interactions in adsorbed SA layer at the liquid/liquid interface since both Eqs. [7] and [18] yield interesting pieces of information, but none of them gives a perfect description of the phenomenon.

The low D values for SA further suggest the presence of an energy barrier of adsorption between the subsurface and the oil/water interface. This barrier might be attributed to the steric restraints on the stearic acid molecules, in the proximity of the oil/water interface, and therefore, the molecules need to achieve a correct orientation to adsorb at the interface. This barrier of adsorption can be also due to a slow reorientation of the

polar head groups of SA molecules at the oil/water interface. This will cause an increase in the timescale for the dynamic interfacial pressure to reach out its equilibrium value.

Eq. [18] proposed in the present paper is better than Eq. [6] and it allows a more correct description of the experimental data of the dynamic interfacial pressures for a large interval of surfactant concentrations in oil solutions and over a period of time that can range up to two hours, depending on the stearic acid bulk concentration. In this period of time, the dynamic interfacial tension, σ(t), will decay to reach its equilibrium value and, consequently, the dynamic interfacial pressure, Π(t), will increase to attain its equilibrium value.

In future studies we intend to extend this investigation by using the diffusion adsorption theory associated with the surface reorientation of the fatty acid molecules at the oil/water interface.

REFERENCES

1. F. Ravera, M. Ferrari and L.Liggieri, *Adv. Colloid Interface Sci.,* **2000***,* 88, 129.
2. J. Eastoe and J. S. Dalton, *Adv. Colloid Interface* Sci., **2000,** 85, 103.
3. B. A. Noskov, *Adv. Colloid Interface* Sci., **1996,** 69, 63.
4. C. -H. Chang and E. I. Franses, *Colloids Surf. A*, **1995**, 100, 1.
5. A. F. H. Ward and L. Tordai, *J. Chem.* Phys., **1946,** 14, 453.
6. P. Joos, G. Bleys and G. Petre, *J. Chim. Phys*., **1982**, 79, 387.
7. G. Bleys and P. Joos, *J. Phys. Chem.,* **1985***,* 89, 1027.
8. P. Joos and G. Serrien, *J. Colloid Interface* Sci., **1989**,127, 97.
9. V. B. Fainerman, S. A. Zholob, R. Miller and P. Joos, *Colloids Surf. A*, **1998**,143, 243.
10. R. Van den Bogaert and P. Joos, *J. Phys. Chem*., **1979,** 83, 2244.
11. R. Van den Bogaert and P. Joos, *J. Phys. Chem*., **1980***,* 84**,** 190.
12. E. Rillaerts, and P. Joos, *J. Colloid Interface* Sci., **1982,** 88, 1.
13. K. A. Coltharp and E. I. Franses, *Colloids Surf. A,* **1996,** 108, 225.
14. K. Theander and R. J. Pugh, *J. Colloid Interface Sci.*, **2001,** 239, 209.
15. G. Czichocki, A.V. Makievski, V. B. Fainerman and R. Miller, *Colloids Surf. A*, **1997**,122, 189.
16. M. Vermeulen and P. Joos, *Colloids* Surf., **1988***,* 33, 337.
17. G. Tomoaia, A. Tomoaia-Cotisel, M. Tomoaia-Cotisel and A. Mocanu, *Cent. Eur. J. Chem.,* **2005**, 3, 347.
18. L. Liggieri, F. Ravera and A. Passerone, *J. Colloid Interface Sci*., **1995***,* 169**,** 238.
19. J. Li, R. Miller and H .Mohwald, *Colloids Surf. A,* **1996,** 114, 113.
20. J. Li, V. B. Fainerman and R. Miller, *Langmuir,* **1996,** 12, 5138.
21. C. J. Beverung, C. J. Radke and H. W. Blanch, *Biophys. Chem*., **1999***,* 81, 59.
22. J. F. Baret, *J. Chim. Phys*., **1968,** 65, 895.

23. E. Chifu, M. Salajan, J. Demeter-Vodnár and M. Tomoaia-Cotisel, *Rev. Roum. Chim*., **1987***,* 32, 683.
24. M. Tomoaia-Cotisel, J. Zsako, G. Tomoaia, A. Mocanu, V. D. Pop, and E. Chifu, *Rev. Roum. Chim*., **2004,** 49, 443.
25. J. Chatterjee and D. T. Wasan, *Chem. Eng. Sci*., **1998,** 53, 2711.
26. L. Liggieri, F. Ravera and A. Passerone, *Colloids Surf. A,* **1996,** 114, 351.
27. F. Ravera, L. Liggieri and A. Steinchen, *J. Colloid Interface* Sci., **1993***,* 156**,** 109.
28. A. Yousef and B. J. McCoy, *J. Colloid Interface Sci.,* **1983,** 94**,** 497.
29. M. Tomoaia-Cotisel, J. Zsako, A. Mocanu, M. Lupea and E. Chifu, *J. Colloid Interface* Sci., **1987***,* 117, 464.
30. J. Zsako, M. Tomoaia-Cotisel, E. Chifu, A. Mocanu and P. T. Frangopol, *Biochim. Biophys. Acta,* **1990,** 1024, 227.
31. M.Tomoaia-Cotisel, *Progr. Colloid Polym.* Sci., **1990**, 83, 155.
32. M. Tomoaia-Cotisel and D. A. Cadenhead, *Langmuir,* **1991**, 7, 964.
33. L. J. Noe, M. Tomoaia-Cotisel, M. Casstevens and P. N. Prasad, *Thin Solid Films*, **1992,** 208, 274.
34. Z. Lu, B. Zhang, Z. Ai, J. Huang and H. Nakahara, *Thin Solid Films,* **1996,** 284-285**,** 127.
35. E. Gyorvary, J. Peltonen, M. Linden and J. B. Rosenholm, *Thin Solid Films,* **1996.** 284-285**,** 368.
36. E. Chifu, M. Tomoaia and A. Ioanette, *Gazz. Chim.* Ital., **1975***,* 105, 1225.
37. R., Miller, P. Joos and V. B. Fainerman, *Adv. Colloid Interface* Sci., **1994***,* 49, 249.
38. A. Sanfeld, A. Steinchen and R. Defay, *J. Phys. Chem*., **1969**, 73, 4047.
39. J. Guastalla, *J. Chim. Phys.,* **1946**, 43, 184.
40. E. Ter Minassian-Saraga, *J. Chim.* Phys., **1955***,* 52, 80.
41. E. Chifu, J. Zsakó and M. Tomoaia-Cotisel, *J. Colloid Interface* Sci., **1983**, 95, 346.
42. M. Tomoaia-Cotisel, E. Chifu, A. Mocanu, J. Zsakó, M. Salajan and P.T. Frangopol, *Rev. Roum.* Biochim., **1988***,* 25, 227.
43. M. Tomoaia-Cotisel, J. Zsako, A. Mocanu, M. Salajan, Cs. Racz, S., Bran and E. Chifu, *Stud. Univ. Babes-Bolyai, Chem*., **2003***,* 48*,* 201.
44. V. G. Babak and F. Boury, *Colloids Surfaces A: Physicochem. Eng. Aspects,* **2004**, 243, 33.
45. M. Tomoaia-Cotisel and P. Joos, *Rev. Roumaine Chim*., **2004,** 49, 539.
46. M. Tomoaia-Cotisel and P. Joos, *Studia, Univ. Babes-Bolyai, Chem*., **2004***,* 49 (1), 35.
47. P. Joos, A. Tomoaia-Cotisel, A. J. Sellers and M. Tomoaia-Cotisel, *Colloids Surfaces. B. Biointerfaces,* **2004,** 37, 83.